

from the master to the slave, and the gain G_2 is responsible for the treatment of the reference signal, which is usually generated by the operator of the master robot. $\{R_m\}$ is used in this case to reflect the environment force sensed by the slave to the master.

In [2] authors presented a first approach to the analysis of stability of the controlled system with time delay, and an analysis of its robustness through the simulation of a range of values for the parameters of the system. Also, authors presented experimental results using a teleoperation system of 1-DOF, i.e. a **SISO** system with 2 states. This technique was originally applicable to systems in which the master and the slave can be modeled by differential equations of the same order, restriction that was overcome in [3] using a discrete approach and concluding that the order of the smaller discrete transfer function (DTF) must be increased up to the order of the other DTF. Simulation results using the discrete approach are presented in [4] for a manipulator of 6-DOF, however, the states-convergence control is applied only to 1-DOF, being the end effector bilaterally controlled.

Other improvements that have been developed have to do with the transparency of the system, which, in the context of bilateral control systems, means that the impedance reflected upon the operator of the master is equal to the impedance of the environment of the slave. In [5], the set of equations required to include the transparency condition in the schema of control by state convergence, is theoretically derived, whereas in [6] authors presented a suitable modification of the schema and showed results of simulations of a 1-DOF system.

A problem arises when having a master and slave with different kinematics because the states-convergence methodology is designed for equal master-slave robots. A solution is figured out in [7] by including a virtual master, who works as a fictitious master simulating the existence of a real one which has the same model and kinematics of the real slave, and interconnecting them as needed by states-convergence control. Once the classical schema has been set between the virtual master and the real slave, a transformation is performed from the kinematics of the real master to the kinematics of the virtual master, thus having an increased schema, where the virtual master is transparent to the operator. In case of having a multiple DOF robot, [7] proposes to set a state space model for each joint, and apply states convergence control to each DOF independently.

A study of the effects of the zeros of the system is presented in [8], where authors showed satisfactory results of the experimentation with a test bench of 1-DOF, and pointed out that in the case of an industrial manipulator, a control system must be designed for each DOF, i.e. solving the **MIMO** control problem through the implementation of a **SISO** controller for each input-output pair. This is known as decentralized **MIMO** control, however, it is well known from the classical control theory that this approach has a good performance only when the system does not present coupling. In those more complex cases as in coupled **MIMO** systems, it becomes necessary to extend the theory in order

to be able to apply control by states convergence.

III. CONTROL BY STATE CONVERGENCE FOR MIMO SYSTEMS WITH TIME DELAY

The proposed control strategy for MIMO systems is compounded into two levels of control: (1) local control for both master and slave sides, which takes care of the coupling problems through a decoupling network and uses states feedback to stabilize and control the robot; and (2), a bilateral control based on the states convergence approach. The complete diagram of the proposed control is shown in Fig.2, where the local control, consisting of the decoupling network and the states feedback are framed as master and slave, while the bilateral control is represented by the interconnection between both systems.

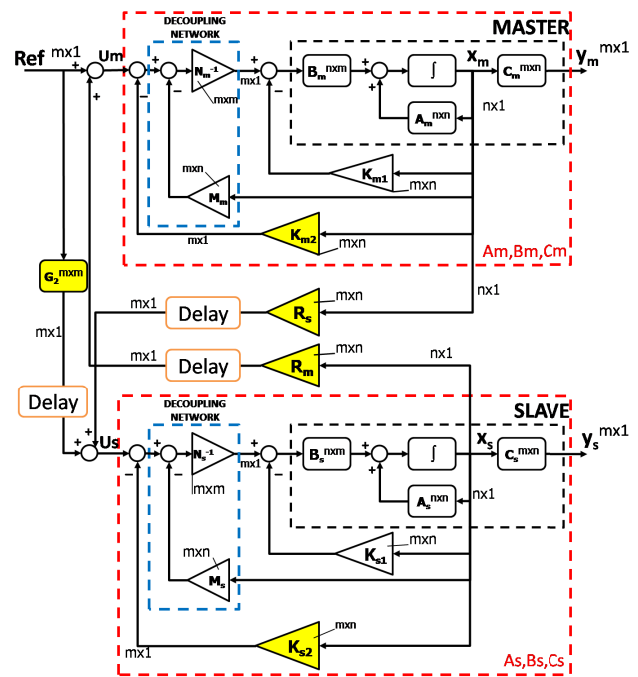


Fig. 2. Proposed control scheme for MIMO systems

The local control must be designed as the first step. The decoupling network is based on the integral decoupling technique presented in [9]. In order to make this paper self contained, the methodology for the design of the decoupling network is briefly presented:

- The plant must be stable. Otherwise, it will be necessary to replace the poles of the plant through the use of states feedback. This is the purpose of K_{m1} and K_{s1} in Fig.2.
- Denoting C_i as the i -th row of the state space matrix C , the derivative of every output of the system can be written as (1)

$$\dot{y}_i = C_i \dot{X} = C_i AX + C_i BU \quad (1)$$

If $C_i B$ is zero, the method developed in [9] indicates to derive (1) until obtain a non null relation between y_i and U . It becomes necessary to perform this procedure

for each output y_i , being the decoupling index d_i the number of derivatives performed for the output y_i .

- Finally, it is obtained a equation of the form,

$$\begin{bmatrix} y_1^{d_1} \\ \vdots \\ y_m^{d_m} \end{bmatrix} = \begin{bmatrix} C_1 A^{d_1} \\ \vdots \\ C_m A^{d_m} \end{bmatrix} \mathbf{x} + \begin{bmatrix} C_1 A^{d_1-1} B \\ \vdots \\ C_m A^{d_m-1} B \end{bmatrix} \mathbf{u} \quad (2)$$

or in its compact form,

$$\tilde{y} = M\mathbf{x} + N\mathbf{u} \quad (3)$$

where M and $Ni = N^{-1}$ are the parameters of the decoupling network.

- Notice that the design procedure requires the existence of N^{-1} , however, there is no such way of assuring its existence before performing the complete calculation.

A decoupling network has been inserted in both the master and in the slave using $\{M_m, N_{im}\}$ and $\{M_s, N_{is}\}$, respectively, as seen in Fig.2. The other part of the local control is states feedback, which has been included using K_{m2} and K_{s2} . These gains can be used to replace the poles of the decoupled system. In order to include the local control (decoupling network and states-feedback) in the state space model, the corresponding matrixes are defined as:

$$\begin{aligned} A_m &= A - BK_{m1} - BN_{im}M_m - BN_{im}K_{m2} \\ B_m &= BN_{im} \\ C_m &= C \\ A_s &= A - BK_{s1} - BN_{is}M_s - BN_{is}K_{s2} \\ B_s &= BN_{is} \\ C_s &= C \end{aligned} \quad (4)$$

Considering the master and the slave as MIMO systems, with n states, m inputs and m outputs, the state space models are specified in (5):

$$\begin{aligned} \dot{X}_m &= A_m X_m + B_m U_m \\ Y_m &= C_m X_m \\ \dot{X}_s &= A_s X_s + B_s U_s \\ Y_s &= C_s X_s \end{aligned} \quad (5)$$

Using this schema and taking into account the number of states and inputs-outputs of the systems, which must be equal for both master and slave, the dimensions of the variables involved in the problem are:

$$\begin{aligned} A_m, A_s &\in \mathbb{R}^{n \times n} \\ B_m, B_s &\in \mathbb{R}^{n \times m} \\ C_m, C_s &\in \mathbb{R}^{m \times n} \\ R_m, R_s &\in \mathbb{R}^{m \times n} \\ G_2 &\in \mathbb{R}^{m \times m} \\ K_{m1}, K_{m2}, K_{s1}, K_{s2} &\in \mathbb{R}^{m \times n} \\ (\text{Decoupling parameter}) M_m, M_s &\in \mathbb{R}^{m \times n} \\ (\text{Decoupling parameter}) N_{im}, N_{is} &\in \mathbb{R}^{m \times m} \end{aligned}$$

U_m and U_s are the external control signals of the master and the slave, respectively. These control signals are determined by the proposed feedback interconnection between both systems for control by states convergence, which is shown in Fig.2. Using a first order Taylor expansion for the delayed signals, with time delay T , U_m and U_s are:

$$\begin{aligned} U_m &= R_m X_s - TR_m \dot{X}_s + Ref \\ U_s &= R_s X_m - TR_s \dot{X}_m + G_2 Ref - TG_2 \dot{Ref} \end{aligned} \quad (6)$$

Considering the reference in steady state, i.e. $\dot{Ref} = 0$, and substituting (6) in (5), we could obtain a new system with states X_s and X_m , as shown in (7)

$$\begin{bmatrix} \dot{X}_s \\ \dot{X}_m \end{bmatrix} = \begin{bmatrix} SA_s & SB_s R_s \\ MB_m R_m & MA_m \end{bmatrix} \begin{bmatrix} X_s \\ X_m \end{bmatrix} + \begin{bmatrix} SB_s G_2 \\ MB_m \end{bmatrix} \mathbf{Ref} \quad (7)$$

or more compact:

$$\begin{bmatrix} \dot{X}_s \\ \dot{X}_m \end{bmatrix} = \hat{A} \begin{bmatrix} X_s \\ X_m \end{bmatrix} + \hat{B} \mathbf{Ref} \quad (8)$$

where $M = (I_{n \times n} + TB_m R_m)^{-1}$, $S = (I_{n \times n} + TB_s R_s)^{-1}$.

Applying the following linear transformation to (8),

$$\begin{bmatrix} \dot{X}_s \\ \dot{X}_e \end{bmatrix} = \begin{bmatrix} I & 0 \\ I & -I \end{bmatrix} \hat{A} \begin{bmatrix} I & 0 \\ I & -I \end{bmatrix} \begin{bmatrix} X_s \\ X_m \end{bmatrix} + \begin{bmatrix} I & 0 \\ I & -I \end{bmatrix} \hat{B} \mathbf{Ref} \quad (9)$$

it is possible to obtain another state space representation of a system whose states are X_s and $X_e = X_s - X_m$, as shown in (10). This last state X_e is the error between the states of the master and the slave.

$$\begin{aligned} \begin{bmatrix} \dot{X}_s \\ \dot{X}_e \end{bmatrix} &= \begin{bmatrix} \hat{A}_{11} + \hat{A}_{12} & -\hat{A}_{12} \\ \hat{A}_{11} - \hat{A}_{21} + \hat{A}_{12} - \hat{A}_{22} & -\hat{A}_{12} + \hat{A}_{22} \end{bmatrix} \begin{bmatrix} X_s \\ X_e \end{bmatrix} \\ &+ \begin{bmatrix} \hat{B}_1 \\ \hat{B}_1 - \hat{B}_2 \end{bmatrix} \mathbf{Ref} \\ \begin{bmatrix} \dot{X}_s \\ \dot{X}_e \end{bmatrix} &= \tilde{A} \begin{bmatrix} X_s \\ X_e \end{bmatrix} + \tilde{B} \mathbf{Ref} \end{aligned} \quad (10)$$

The system that has been obtained in (10) contains the key information for control by states convergence that will be used in the following sections for deriving the design conditions.

A. Master-Slave Error

From (10) it is determined that:

$$\begin{aligned} \dot{X}_e &= (\hat{A}_{11} - \hat{A}_{21} + \hat{A}_{12} - \hat{A}_{22})X_s \\ &+ (-\hat{A}_{12} + \hat{A}_{22})X_e \\ &+ (\hat{B}_1 - \hat{B}_2)Ref \end{aligned} \quad (11)$$

where it is observed that if,

$$\tilde{A}_{21} = 0 = \hat{A}_{11} - \hat{A}_{21} + \hat{A}_{12} - \hat{A}_{22} \quad (12)$$

$$\tilde{B}_2 = 0 = \hat{B}_1 - \hat{B}_2 \quad (13)$$

the error will evolve as an autonomous system, independently of X_m and X_s .

B. System Dynamics

The system dynamics can be studied using the transfer function

$$G(s)_{2n \times m} = C_{2n \times 2n} \{sI_{2n \times 2n} - \tilde{A}_{2n \times 2n}\}^{-1} \tilde{B}_{2n \times m} \quad (14)$$

$$\begin{aligned} G(s)_{2n \times m} &= \frac{1}{\det[sI_{2n \times 2n} - \tilde{A}_{2n \times 2n}]} \times C_{2n \times 2n} \\ &\times \begin{bmatrix} sI_{n \times n} - \tilde{A}_{22n \times n} & \hat{A}_{12n \times n} \\ [0]_{n \times n} & sI - \hat{A}_{11n \times n} \end{bmatrix} \\ &\times \begin{bmatrix} B_{m \times m} \\ [0]_{n \times m} \end{bmatrix} \end{aligned} \quad (15)$$

where the presence of the null matrixes is due to the conditions in (12) and (13). Therefore the characteristic equation of $G(s)$ is $\det[sI_{2n \times 2n} - \tilde{A}_{2n \times 2n}]$, and using the Leibnitz formula for the determinant of a square matrix, it can be rewritten as:

$$\det[sI_{n \times n} - \tilde{A}_{11_{n \times n}}] \det[sI_{n \times n} - \tilde{A}_{22_{n \times n}}] = 0 \quad (16)$$

where each determinant is a polynomial of n -th order with respect to s . The first determinant fixes the slave dynamics, while the second one determines the error dynamics.

C. Design conditions for MIMO case

Conditions (17) and (18), previously derived, must be obligatory satisfied in order to achieve state convergence, while (19) and (20) can be used to manipulate the slave and error dynamics depending of the design criteria, by selecting the coefficients $\{a_{n-1}, \dots, a_1, a_0\}$ and $\{b_{n-1}, \dots, b_1, b_0\}$ that provides the desired poles.

$$\tilde{A}_{21} = 0 = \hat{A}_{11} - \hat{A}_{21} + \hat{A}_{12} - \hat{A}_{22} \quad (17)$$

$$\tilde{B}_2 = 0 = \hat{B}_1 - \hat{B}_2 \quad (18)$$

$$\det[sI_{n \times n} - \tilde{A}_{11_{n \times n}}] = s^n + a_{n-1}s^{n-1} + \dots + a_1s + a_0 \quad (19)$$

$$\det[sI_{n \times n} - \tilde{A}_{22_{n \times n}}] = s^n + b_{n-1}s^{n-1} + \dots + b_1s + b_0 \quad (20)$$

When including the local control ((4) and (7)) in the set of conditions (17), (18), (19) and (20), we obtain the following set of equations,

$$\begin{aligned} (I_{n \times n} + TB_s R_s)^{-1} (A_s + B_s R_s) \\ - (I_{n \times n} + TB_m R_m)^{-1} (B_m R_m + A_m) = [0]_{n \times n} \end{aligned} \quad (21)$$

$$(I_{n \times n} + TB_s R_s)^{-1} B_s G_2 - (I_{n \times n} + TB_m R_m)^{-1} B_m = [0]_{n \times n} \quad (22)$$

$$\begin{aligned} \det[sI_{n \times n} - (I_{n \times n} + TB_m R_m)^{-1} A_m + (I_{n \times n} + TB_s R_s)^{-1} B_s R_s] \\ = s^n + a_{n-1}s^{n-1} + \dots + a_1s + a_0 \end{aligned} \quad (23)$$

$$\begin{aligned} \det[sI_{n \times n} - (I_{n \times n} + TB_s R_s)^{-1} (A_s + B_s R_s)] \\ = s^n + b_{n-1}s^{n-1} + \dots + b_1s + b_0 \end{aligned} \quad (24)$$

Up to this point, all the required equations have been derived for the design of the control by states convergence proposed in Fig.2. Due to the nature of the conditions, (21), (22), (23) and (24) constitutes a set of $((m \times n) + (m \times m) + 2n)$, where the state-convergence conditions (21) and (22) contribute with $(m \times n)$ and $(m \times m)$ equations, respectively, while (23) and (24) contribute with n equations each one. Notice that when $m = 1$, which is the **SISO** case, the number of equations is reduced to $(3n + 1)$, fact that coincides with the results obtained in [1]. On the other hand, the set of control parameters is compounded by $\{K_{m2} \in \mathbb{R}^{m \times n}, K_{s2} \in \mathbb{R}^{m \times n}, R_m \in \mathbb{R}^{m \times n}, R_s \in \mathbb{R}^{m \times n}, G_2 \in \mathbb{R}^{m \times m}\}$. This paper proposes the next solution to the problem that has been formulated:

- Fix K_{m2} and K_{s2} when designing the local control, and then solving (21), (22) and (23) for $R_m \in \mathbb{R}^{m \times n}, R_s \in \mathbb{R}^{m \times n}, G_2 \in \mathbb{R}^{m \times m}$, which

supposes an excess of $((m - 1) \times n)$ parameters to be fixed, this issue can be solved, without losing generality in the solution, by arbitrarily setting to zero $((m - 1) \times n)$ elements into the variables' matrixes. Notice that this is valid for $m \geq 1$, which is always satisfied by a **MIMO** system. The final location of the master and slave poles must be reviewed in order to assure the stability of the system.

There are other ways of finding a solution to this set of equations, however it is out of the scope of this paper due to the complexity of the nonlinear equations that arise when solving the four conditions simultaneously for $\{K_{s2} \in \mathbb{R}^{m \times n}, R_m \in \mathbb{R}^{m \times n}, R_s \in \mathbb{R}^{m \times n}, G_2 \in \mathbb{R}^{m \times m}\}$, in which case, an excess of $(2(m - 1) \times n)$. The methodology proposed presents less complicated nonlinear equations, that allows to establish the desired dynamics of the error between master-slave states.

IV. TELEOPERATION OF A 2-DOF HELICOPTER

The **MIMO** control strategy was assessed by applying it to the 2-DOF helicopter commercial platform of QUANSER, as the one showed in Fig.3. This platform counts with two DC motors mounted at the two ends of a rectangular frame and drive two propellers. The controlled variables are the pitch angle θ , and the yaw angle ψ , while the control signals are the voltages of the two DC motors.

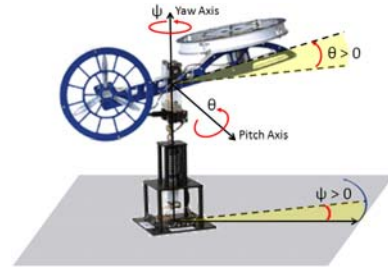


Fig. 3. 2-DOF Helicopter

The state space model provided by QUANSER is in (25), with four states ($n = 4$): pitch angle θ , yaw angle ψ , pitch angular velocity $\dot{\theta}$, and yaw angular velocity $\dot{\psi}$.

$$\begin{aligned} \dot{\mathbf{x}} &= \begin{bmatrix} 0 & 0 & 1 & 0 \\ 0 & 0 & 0 & 1 \\ 0 & 0 & -\frac{B_p}{J_{eq,p+m_{heli}l_{cm}^2}} & 0 \\ 0 & 0 & 0 & -\frac{B_y}{J_{eq,y+m_{heli}l_{cm}^2}} \end{bmatrix} \mathbf{x} \\ &+ \begin{bmatrix} 0 & 0 \\ 0 & 0 \\ \frac{K_{pp}}{J_{eq,p+m_{heli}l_{cm}^2}} & \frac{K_{py}}{J_{eq,p+m_{heli}l_{cm}^2}} \\ \frac{K_{yp}}{J_{eq,y+m_{heli}l_{cm}^2}} & \frac{K_{yy}}{J_{eq,y+m_{heli}l_{cm}^2}} \end{bmatrix} \mathbf{u} \\ \mathbf{y} &= \begin{bmatrix} 1 & 0 & 0 & 0 \\ 0 & 1 & 0 & 0 \\ 0 & 0 & 0 & 0 \\ 0 & 0 & 0 & 0 \end{bmatrix} \mathbf{x} \end{aligned} \quad (25)$$

where m_{heli} is the mass of the helicopter, l is the distance from the yaw axis to center of mass of the helicopter, $J_{eq,p}$ and $J_{eq,y}$ are the equivalent moments of inertia with respect of the pitch and yaw axis, respectively; and K_{ab}

denotes the thrust torque constant acting on a axis from b motor/propeller, being a and b the pitch and yaw depending on the case.

The system presents coupling between θ and ψ , as it can be concluded from the step responses when the system is only stabilized through states feedback. The step response in this situation is presented in Fig.4, from which it can be noticed that the step for the pitch angle at $t = 10\text{sec}$ affects the yaw angle, and viceversa in the case of the step for the yaw angle at $t = 20\text{sec}$. Notice that the cross effect of θ over ψ is bigger than the contrary effect. This problem is solved using the decoupling network designed for this system, which has decoupling index $d = 2$, for both outputs.

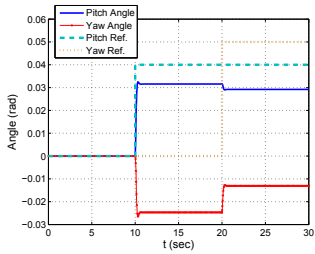


Fig. 4. Coupling tests of the stabilized system

Due to its **MIMO** nature and the coupling that is usually present in aerial vehicles, this test bench has been considered a good platform for testing the control strategy, moreover, it has been considered a contribution to the state of the art in control by states convergence, because it has been applied in the past only to manipulators and using 1-DOF.

Several tests were performed in simulation using Matlab®/Simulink®, where the master is the simulation of the state space model of the 2-DOF helicopter, while the slave is a simulation of its nonlinear model. This structure for the simulation was designed in order to make the simulation closer to the real teleoperation, in which the human operator could use a joystick, and then perform a kinematics transformation to a virtual master (simulation of the 2-DOF helicopter) which is similar and is coupled to the real slave through the schema of state convergence control, as proposed in [7] and illustrated in Fig.5. The following section shows the results that correspond to the framed section marked as *Bilateral Control by State Convergence* in Fig.5, with a simulation of the slave; this section of the diagram represents the main theory presented in this paper.

V. RESULTS

The goal of the tests was to observe the response of the teleoperation system in different situations. The first result presented in Fig.6 correspond to a master-slave following case, in which the operator changes the reference of the system for both pitch and yaw angles. Notice that the initial condition of the platform is always $\{\theta = -0.75\text{rad}, \psi = 0\text{rad}\}$, due to the localization of the center of mass of the helicopter with respect to the yaw axis. In Fig.6(a) is presented

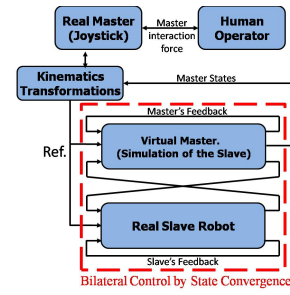
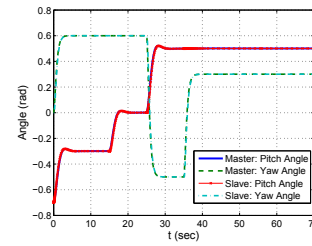
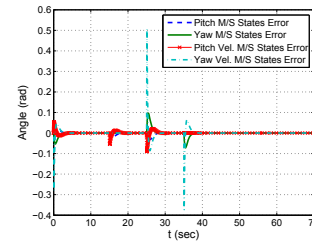


Fig. 5. Teleoperation schema when having master-slave with different kinematics

the response of the yaw and pitch angle, when the reference is a steps sequence for pitch of the form: $\{-0.3\text{rad for } [0\text{sec} \leq t \leq 15\text{sec}], 0\text{rad for } [15\text{sec} < t \leq 25\text{sec}], 0.5\text{rad for } [25\text{sec} < t \leq 70\text{sec}]\}$, while the yaw angle reference is of the form: $\{0.6\text{rad for } [0\text{sec} \leq t \leq 25\text{sec}], -0.5\text{rad for } [25\text{sec} < t \leq 35\text{sec}], 0.3\text{rad for } [35\text{sec} < t \leq 70\text{sec}]\}$. The time delay is 1msec . This experiment is useful to show that the decoupling network has eliminated the cross effect that the helicopter presented in Fig.4.



(a) Pitch and yaw angles



(b) Master-Slave states error

Fig. 6. Master-slave following case

On the other hand, the master-slave tracking task was performed satisfactorily. Fig.6(b) presents the response of the master-slave states error, which has shown convergence to zero in steady state, as expected from conditions (17) and (18), that were satisfied by the numerical method-based solution up to a error tolerance of 10^{-18} .

In order to give a better illustration of the time delay effect, the system was excited with a pulse train for pitch angle, in presence of a 10msec time delay. The response is showed in Fig.7, with a zoom that allows to observe the delayed tracking.

Besides the tracking tests, it is important to analyze

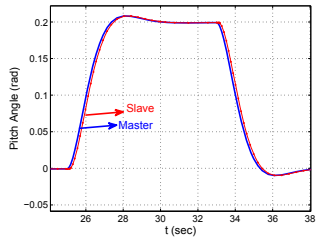


Fig. 7. Test

the effects of disturbances caused by the environment of the slave. For this reason, a simulation was performed in which the reference for pitch angle is $\{0\text{rad for } [0\text{sec} \leq t \leq 15\text{sec}], 0.5\text{rad for } [15\text{sec} < t \leq 40\text{sec}]\}$, while the yaw angle reference is $\{0\text{rad for } [0\text{sec} \leq t \leq 5\text{sec}], 0.3\text{rad for } [5\text{sec} < t \leq 40\text{sec}]\}$. Time-limited disturbances in the slave were added as follows: $\{0.1\text{rad for } [5\text{sec} < t \leq 6\text{sec}]\}$ for yaw angle, and $\{0.1\text{rad for } [25\text{sec} \leq t \leq 26\text{sec}]\}$ for pitch angle. Results are shown in Fig.8.

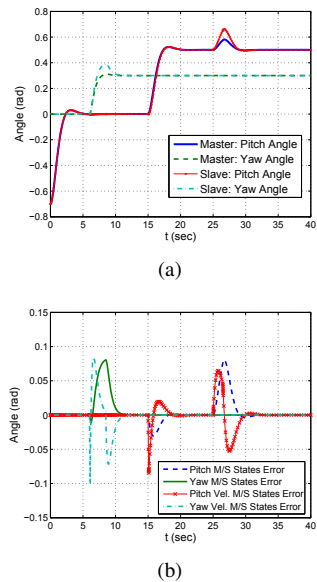


Fig. 8. Response of the system under disturbances in the environment of the slave

Based on Fig.8(a), notice how the disturbances in the environment of the slave directly affects the slave output, as well as its states (Fig.8(b)), and are reflected to the states of the master. The result obtained shows major impact in the slave device than in the master, having the same waveform and duration, but less amplitude in the master side. The transparency of the bilateral control system could be improved by developing its conditions for the **MIMO** case.

VI. CONCLUSIONS

The generalization of the theory of bilateral control by states convergence to **MIMO** systems has been presented, considering the coupling problem and the time delay in the

master-slave communication channels. The proposed strategy includes a *local control* compounded by a decoupling network and control by states feedback, and a *bilateral control* compounded by a set of feedback connections between the master and the slave that allow to achieve states convergence, so that the slave can follow the master, in spite of time delay and disturbances that could affect the control system. In this paper, the local control is based on a decoupling technique, but it can be designed using another control strategy.

A set of four conditions was presented, two of them must be obligatory satisfied since they guarantee that the error between master-slave states will evolve as an autonomous system, while the other two conditions are related to the dynamics of the slave and the error, and can be used any which way the designer selects. These four conditions are similar to those in the **SISO** case because they are derived directly from the state convergence core, however, when including the information about the control signals and the dimensions of the systems, a set of $((m \times n) + (m \times m) + 2n)$ nonlinear equations are obtained, which comes from the proposed m-inputs, m-outputs, n-states **MIMO** schema. An application to the teleoperation of a 2-DOF helicopter is developed through simulation. The decoupling network and the states feedback local control were designed from the state space model of the 2-DOF helicopter, whereas the control parameters for states convergence were obtained by solving a set of equations for the autonomous evolution of the error and the error dynamics, using numerical methods. Simulations exhibit satisfactory performance. This work has potential for future applications in the teleoperation of unmanned aerial vehicles (UAV), and future work will be focused on experimentation with a real slave helicopter.

REFERENCES

- [1] J. M. Azorín, O. Reinosoa, R. Aracil, and M. Ferre, "Generalized control method by state convergence for teleoperation systems with time delay," *Automatica*, vol. 40, no. 9, pp. 1575–1582, 2004.
- [2] J. M. Azorín, O. Reinosoa, R. Aracil, and M. Ferre, "Control of teleoperators with communication time delay through state convergence," *Journal of Robotic Systems*, vol. 21, no. 4, pp. 167–182, 2004.
- [3] J. M. Azorín, R. Aracil, J. M. Sabater, M. Ferre, N. M. García, and C. Pérez, "Bilateral control of different order teleoperators," *Springer Tracts in Advanced Robotics*, vol. 22, pp. 119–127, 2006.
- [4] J. Barrio, J. M. Azorín, R. Aracil, M. Ferre, and J. N. M. G. J. M. Sabater, "Experimental bilateral control by state convergence," in *Proc. IEEE/RSJ International Conference on Intelligent Robots and Systems (IROS'06)*, Beijing, China, Oct. 2006, pp. 1127–1132.
- [5] J. M. Bogado, M. Ferre, R. Aracil, J. M. Azorín, E. M. Fernández, and J. Baca, "Transparency analysis of bilateral controllers based on the methodology of state convergence," in *Haptics: Perception, Devices and Scenarios - LNCS*, vol. 5024, Madrid, Spain, June 2008, pp. 122–128.
- [6] J. M. Azorín, R. Aracil, C. Pérez, N. M. García, and J. M. Sabater, "Transparent bilateral control for time-delayed teleoperation by state convergence," in *Proc. IEEE International Conference on Robotics and Automation (ICRA 2008)*, Pasadena, U.S.A., May 2008, pp. 643–648.
- [7] C. Peña, R. Aracil, and R. Saltarén, "Teleoperation of a robot using a haptic device with different kinematics," in *Haptics: Perception, Devices and Scenarios - LNCS*, vol. 5024, Madrid, Spain, 2008, pp. 181–186.
- [8] J. M. Azorín, R. Aracil, J. M. Sabater, M. Ferre, N. M. García, and C. Pérez, "Bilateral control of teleoperation systems through state convergence," *Advances in Telerobotics. Springer Tracts in Advanced Robotics*, vol. 31, pp. 271–278, 2007.
- [9] W. Falb, P. Wolovich, "Decoupling in the design and synthesis of multivariable control systems," *IEEE Transactions on Automatic Control*, vol. AC-12, pp. 651–659, 1967.